Supplementary Materials for

Targeted Enhancement of Cortical-Hippocampal Brain Networks and Associative Memory

Jane X. Wang, Lynn M. Rogers, Evan Z. Gross, Anthony J. Ryals, Mehmet E. Dokucu, Kelly L. Brandstatt, Molly S. Hermiller, and Joel L. Voss

Correspondence to: joel-voss@northwestern.edu

This section includes:

Materials, Methods and Supplementary Text

Primary Experiment

Subjects

Data are reported from 16 healthy adults (9 female, ages 20-32 years). Incomplete datasets were collected from an additional two individuals (one failed to complete the study and MRI data were incomplete for one), and these datasets were excluded from analyses. No subjects withdrew due to complications from the TMS procedures, and no negative treatment responses were observed. All subjects had normal or correct-to-normal vision and did not report neurological or psychiatric disorders or the current use of psychoactive drugs. All subjects were eligible for MRI and TMS procedures based on standard MRI safety screening as well as on their answers to a TMS safety-screening questionnaire (*27*). All subjects gave written, informed consent and were remunerated for their participation. The study protocol was approved by the Northwestern University Institutional Review Board.

Experiment design

Each subject participated for two weeks, one week with stimulation and one week with sham stimulation, separated by at least 1 week (mean = 2.5 weeks, range 1 - 4 weeks). Each week included baseline, Mid-Tx, and Post-Tx assessments (Fig. 1). The baseline assessment occurred one day prior to the first stimulation session, and there were five consecutive daily stimulation sessions. The Mid-Tx assessment occurred immediately after the third stimulation session, and the Post-Tx assessment occurred one day after the final stimulation session (mean delay = 24.9 h, range = 16-32 h; Fig. 1). The order of the stimulation versus sham weeks was counterbalanced across subjects (i.e., half of subjects received stimulation first and half received sham first).

The following measures were collected for the baseline, Mid-Tx, and Post-Tx assessments for both weeks. Structural MRI and resting-state fMRI were collected for each session using the parameters indicated below. Following MRI scanning, subjects performed an associative memory test (face-cued word recall), a computerized neuropsychological battery, and three self-report mood/affect questionnaires, as described below.

MRI parameters

MRI data were collected at the Northwestern University Center for Translational Imaging using the following parameters. A Siemens 3T TIM Trio whole-body scanner with a 32-channel head coil was used. Head movement was minimized using padding. A structural image was acquired to provide anatomical localization (MPRAGE T_1-weighted scans, TR = 2400 ms, TE = 3.16 ms, voxel size = 1 mm^3, FOV = 25.6 cm, flip angle = 8°, 176 sagittal slices). fMRI was performed using whole-brain BOLD EPI (TR = 2500 ms, TE = 20 ms, voxel size = 1.72 x 1.72 x 3 mm^3, FOV = 22 cm, flip angle = 80°). Each resting-state scan included 244 volumes (10.2 minutes total), collected in sequential order. Subjects were instructed to lie still with their eyes open during resting-state scanning, and ambient lighting was dimmed. MRI scanning was performed before memory testing on each assessment day in order to eliminate any carry-over effects from testing on brain activity during resting-state fMRI.

Identification of stimulation locations and rTMS parameters

We identified a stimulation location for each subject using individual maps of hippocampal resting-state functional connectivity obtained at the baseline assessment at the beginning of the first study week. For each subject, fMRI collected during resting state was used to generate seed-based connectivity maps using a hippocampal target as the seed. The structural MRI for

each subject was transformed into stereotactic space (MNI-305) using AFNI (*28*). The transformation matrix was stored to enable conversion between original MRI space and stereotactic space during analysis and TMS procedures. After transformation, a hippocampal target voxel was located for each subject by identifying the voxel in the middle of the hippocampal body that was nearest to MNI coordinate x=-24, y=-18, z=-18. This MNI coordinate was selected because this location robustly shows functional connectivity with lateral parietal cortex in group-level studies (*8*). We focused on lateral parietal cortex as a stimulation location because it is the portion of the hippocampal intrinsic fMRI connectivity networks that can be best targeted with rTMS (as it is superficial). The only other moderately superficial region that is robustly within the hippocampal fMRI network is medial prefrontal cortex (*4,8*), and we avoided stimulation of this location because the cortical surface is oriented perpendicular to the stimulating coil, and therefore rTMS might be minimally effective for this region. The left hemisphere was selected due to the known role of left lateral parietal cortex in memory retrieval (*7*), and thus the target was located in left hippocampus because hippocampal connectivity with lateral parietal cortex is primarily ipsilateral (*8*). We selected the voxel individually based on structural MRI in order to account for individual differences in hippocampal anatomy (as in (*29*)). The hippocampal targets for each subject are displayed in stereotactic space overlaid on a template brain in Fig. S1.

Functional and structural MRI data were preprocessed using AFNI (31). For the purpose of identifying stimulation targets, preprocessing steps included motion correction, slice-timing correction to the first slice, functional/structural coregistration, resampling to a resolution of 1.5 x 1.5 x 1.5mm^3, stereotactic transformation using the Montreal Neurologic Institute 305 (MNI-305) template, and spatial smoothing with a 4-mm FWHM Gaussian kernel. Following preprocessing, the fMRI timecourse of the hippocampal target was extracted and used for seed-based analysis of resting-state functional connectivity. For this analysis, fMRI timecourse data were bandpass filtered at 0.01 – 0.1 Hz and linearly detrended. We identified the cluster of voxels exhibiting the local maximum connectivity within a 15 mm radius of the MNI coordinate x=-47, y=-68, z=+36 (an area encompassing the inferior parietal lobule (supramarginal and angular gyrus), Brodmann areas 39 and 40). This stimulation location was marked in stereotactic space (Fig. S1), then transformed into original MRI space and overlaid onto the structural MRI to provide localization during rTMS.

rTMS was applied to the stimulation location during daily treatment sessions using a Nexstim eXimia NBS 4.3 air-cooled, MRI-guided system (Nexstim Ltd., Helsinki, Finland). A 70mm figure eight coil was used. Motor threshold was determined for each subject during the baseline assessment at the beginning of the first study week, defined as the minimum stimulator output value required to generate contraction of the *abductor pollicis brevis* for at least 5 of 10 consecutive pulses (measured via EMG using a contraction threshold of 50 mV). For the stimulation condition, rTMS was applied at 100% motor threshold to the stimulation location for 20 minutes of consecutive blocks of 20Hz pulses for two seconds followed by 28 seconds of no stimulation. The stimulation location was targeted via MRI using a frameless infrared stereotactic system. The induced current field was oriented perpendicular/anterior to the long axis of the gyrus encompassing the stimulation location. The estimated induced voltage at the stimulation location was calculated based on a realistic head model (*30*) and recorded for each session. For the sham stimulation condition, rTMS was applied to the same location using the same parameters, except that a spacer was used to increase the distance between the coil and the target such that the estimated induced voltage at the stimulation location was zero (calculated online during TMS delivery). During week 2, subjects could discriminate the stimulation from the sham week based on comparison of stimulation intensity. However, subjects were not aware of hypotheses regarding the effects of different stimulation intensities.

Further, we used group-level comparisons to identify stimulation versus sham effects during week 1, before subjects could discriminate stimulation intensities during week 2 (i.e., comparison of stimulation for subjects receiving stimulation during week 1 (n=8) to sham for subjects receiving sham during week 1 (n=8)). Findings were similar to those for within-subjects comparisons in the entire sample, and are described below in the section on the negative-control experiment.

Associative memory test

Associative memory was tested using face-cued word recall. Subjects studied 20 human face photographs presented individually in grayscale on printed cards for ~3s each. The experimenter read a unique common word aloud when each card was shown. The subject was instructed to memorize the association between the face and the word. After a filled delay of approximately one minute following study, subjects were shown the same 20 faces, individually and in a different randomized order, and attempted to recall the words that were presented with each face at study. Word recall for each face was scored as correct or incorrect (forgiving pronunciation errors including plurality), and performance was calculated as percentage correct out of 20. There were six alternative forms of the test, each using a different set of faces and words, which were assigned to the six assessments using a Latin square. Faces were taken from a database of amateur model headshots (*31*). Each test form included only male faces or only female faces. Words were nouns between 3 and 8 letters in length, had written Kucera-Francis frequencies of between 200 to 2000, and had concreteness ratings of 300 to 700 (identified using the MRC Psycholinguistic Database; www.psych.rl.ac.uk). To account for individual differences in overall performance levels and for variation in performance across weeks, the primary analyses included in the manuscript use change scores versus baseline, whereby the change between each assessment and baseline was expressed as a proportion of baseline performance for each subject and for each week of testing (i.e., Mid-Tx and Post-Tx change from baseline for the stimulation week, and likewise for the sham week). Raw scores for each assessment are provided in Table S2.

Computerized neuropsychological battery

The NIH Toolbox for Cognition (*32*) was administered during each assessment using a laptop computer. There were seven instruments, including: (1) the Flanker Inhibitory Control and Attention Test (for executive function and attention), (2) the Dimensional Change Card Sort Test (for executive function and set shifting), (3) the List Sorting Working Memory Test (for working memory), the Picture Sequence Memory Test (for story sequence memory), the Oral Reading Recognition Test (for language), the Picture Vocabulary Test (for language), and the Pattern Comparison Processing Speed Test (for processing speed). There were three alternative forms of the test used during each week, in randomized order. Notably, although the Picture Sequence Memory Test is ostensibly a measure of memory, there are no data available to evaluate the association between performance and the hippocampus (unlike the face-cued word recall test that was used as the primary memory measure). Furthermore, the test involves relatively short-term (~30 s) retention of a story sequence, and verbal sequencing memory has been associated with prefrontal cortex and prefrontal-hippocampal interactions more so than with the posterior parietal-hippocampal network targeted here (e.g., *33, 34*). We therefore did not predict stimulation effects on this measure. Administration was ~40 minutes for all tests. All subjects were within the normative range of performance (all above 1 SD below the mean) on all tests relative to a large sample of age, gender, race, and education-matched controls (*32*). As reported in the text, there were no significant effects of stimulation identified for any test.

Questionnaire measures of emotion/mood

Emotion/mood was assessed using three of the questionnaire instruments of the Neuro-QOL assessment system, which were administered via computer adaptive testing (*35*). The instruments included questionnaires for depression, fatigue, and anxiety. All subjects were within the normal range for these measures (all above 1 SD below the mean). Notably, a trend-level effect of stimulation was identified for the depression questionnaire only ($P = 0.09$; Fatigue $P = 0.255$, Anxiety $P = 0.59$), although it should be noted that no correction for multiple comparisons was made. Given that all subjects were within the normal range, this finding, if reliable, would indicate a slight reduction in normal levels of negative affect/mood, rather than any alleviation of depression-like symptoms.

Whole-brain fMRI connectivity analysis for the hippocampal target

fMRI preprocessing was similar to that used for identifying stimulation targets, including motion correction, slice-timing correction to the first slice, functional/structural coregistration, resampling, and stereotactic transformation (MNI-305), but did not include spatial smoothing in order to reduce spurious correlations at small distances.

A group mask was defined by masking out ventricular regions, white matter, and areas of the brain perimeter (especially inferior cerebellum) that were not sampled in each subject. Time courses were extracted from all voxels (of size 1.5 x1.5 x 1.5 mm^3) within this mask for every subject. Time series were detrended for linear drift and for estimated motion and bandpass filtered at 0.01 – 0.1 Hz. Volumes with high framewise displacement (> 0.3 mm) were removed (*36*). Subject-specific seed-based connectivity maps were calculated with respect to each individual's hippocampal target. Time series within the target and voxels immediately surrounding it (defined as the intersection of voxels encompassed by a 3mm-radius sphere centered on the target with voxels encompassed by a mask of hippocampus proper; mean volume = 96mm^3) were averaged to generate a seed timeseries, which was subsequently used to calculate seed connectivity maps by calculating the Pearson's correlation value between the seed timeseries and those of all nonseed voxels. One map was created for each of the baseline and Post-Tx sessions for the stimulation and sham weeks. For one subject, Mid-Tx fMRI values for stimulation were used as the stimulation baseline because the stimulation baseline scan was corrupted due to artifact (this would have served to diminish, rather than enhance, the reliability of any observed effects of stimulation).

Group-level statistical maps of T values were calculated for the comparison of connectivity for baseline versus Post-Tx, for stimulation relative to sham (after transforming Pearson's correlation values to Fisher's Z). The voxel-wise threshold was set to $P < 0.05$ and a spatial-extent threshold of 290 contiguous supra-threshold voxels (979 mm^3) was determined via Monte Carlo simulation to provide a combined corrected threshold of $P < 0.05$. For Fig. 2, results were rendered onto the N27 template brain (*37*) using MRIcroN.

Selectivity analysis of fMRI connectivity changes for the hippocampal target

Selectivity for the target site was calculated by translating each subject's hippocampal seed along the anterior-posterior axis of the hippocampus in 1.5 mm increments from -9mm to +9mm (using the center voxel of the hippocampus in the coronal view as the seed for each 1.5-mm step, to account for the curved shape of the hippocampus along the anterior-posterior axis). Note that this analysis treated each individual subject's seed location as the zero point, and anterior/posterior displacements were relative to the individual seed locations. Whole-brain connectivity maps were generated for each of the 12 displaced seed locations along the anterior-posterior axis as described above for the target location. After transformation to Fisher's Z, global averages in connectivity differences were calculated (i.e., mean baseline to Post-Tx

change for all voxels relative to the seed; black line in Fig. 2B). Assessment of global (i.e., whole-brain) fMRI connectivity changes was used to avoid any bias that would result by focusing on a specific region. Connectivity differences were also calculated for the four significant treatment-responsive regions identified in the seed-based analysis (colored lines in Fig. 2C). At the hippocampal targets, robust changes were observed at both the global level (mean change = 0.040, $T_{(15)} = 2.21$, $P = 0.043$) and (by definition) for the four stimulation-responsive regions identified using voxel-based whole-brain analysis and reported in Fig. 2 (retrosplenial/precuneus mean = 0.189, $T_{(15)} = 5.42$, $P < 0.0001$; fusiform/parahippocampal: mean = 0.171, $T_{(15)} = 5.54$, $P < 0.0001$; superior parietal cortex: mean = 0.157, $T_{(15)} = 5.66$, $P < 0.0001$; lateral parietal cortex: mean = 0.157, $T_{(15)} = 5.14$, $P < 0.0005$).

The selectivity of stimulation effects was also tested by calculating changes in fMRI connectivity for the right hippocampus, at locations corresponding to target locations in the left hippocampus (i.e., target locations reflected about the midline to right hippocampus). Robust changes in connectivity were not observed using right hippocampus reflected targets (Post-Tx versus baseline for stimulation relative to sham) for the global connectivity measure (mean change = 0.015, $T_{(15)}=0.41$, $P = 0.689$) or for any of the four stimulation-responsive regions identified in Fig. 2A, with values that are in stark contrast to those observed for hippocampal targets (retrosplenial/precuneus mean = 0.029, $T_{(15)} = 1.01$, $P = 0.327$; fusiform/parahippocampal: mean = 0.058, $T_{(15)} = 2.67$, $P = 0.017$; superior parietal cortex: mean = 0.015, $T_{(15)} = 0.48$, $P = 0.641$; lateral parietal cortex: mean = -0.023, $T_{(15)} = -1.02$, $P = 0.323$), with none of these comparisons surviving correction for multiple comparisons (corrected $\alpha = 0.0125$ for 4 comparisons). This is striking in light of the fact that hippocampal regions along the anterior-posterior axis in each hemisphere tend to show robust fMRI connectivity with their corresponding regions in the contralateral hippocampus, as was the case here for baseline fMRI connectivity. This further supports the disproportionate effects of stimulation to the targeted portion of the hippocampus (and not the same region of contralateral hippocampus). Similarly, there were no significant stimulation-induced changes for the left hippocampus treated as a unit (all P values > 0.35 for the global connectivity measure and for the four regions identified in Fig. 2A), further indicating that stimulation effects were specific to the targeted portion of left hippocampus, and were thus not robust when considering the entire left hippocampus (including the far posterior aspect of hippocampus, which was not fully interrogated in the analysis reported in Fig. 2B).

Analysis of fMRI interconnectivity among treatment-responsive regions

Analyses of fMRI connectivity among treatment-responsive regions (Fig. 3) concerned voxels that demonstrated at least a marginal baseline to Post-Tx fMRI connectivity change for stimulation relative to sham (voxel-wise $P < 0.05$, with no spatial extent threshold) with the hippocampal target (i.e., stimulation-induced change in connectivity with respect to the hippocampal target, but not necessarily with respect to one another). This liberal threshold was used in order to characterize the broader effects of stimulation on regional interconnectivity, without selecting for only those voxels that show the most robust treatment effects. The time series of treatment-responsive voxels were averaged spatially for all voxels within AAL-defined anatomical regions (*38*) and were correlated against each other to give a correlated-weighted fMRI connectivity matrix (Fig. 3A). AAL regions were only included if they included > 20 treatment-responsive voxels, in order to reduce the influence of spurious correlations on findings. Overall, the effects of treatment on regional interconnectivity were highly robust, with 405 interregional links (15.8% of total) surviving FDR correction (Fig. S2). The matrix in Fig. 3A was ordered such that rows and columns at the top and left of the matrix reflected regions with higher baseline connectivity with hippocampal targets, in order to permit visualization of the relationship between increases in regional interconnectivity and extent of inclusion in baseline hippocampal fMRI connectivity networks. Notably, the significant relationship between degree of

connectivity with the hippocampal target at baseline and amount of regional interconnectivity increase due to stimulation (Fig. 3B) was robust even when all AAL regions were included in the analysis (i.e., including those with ≤ 20 treatment-responsive voxels; $R^2_{(adj)} = 0.32$, df = 86, P < 0.0001), indicating that the reported effects are robust to this analysis parameter.

To test the selectivity of this effect to hippocampal targets versus the parietal stimulation locations, an additional analysis was performed to assess the relationship between degree of connectivity with the parietal locations at baseline and amount of interconnectivity increase due to stimulation. There was no significant relationship between the number of significant links and baseline connectivity with parietal stimulation locations using the same analysis as in Fig. 3B ($R^2_{(adj)} = 0.02$, df = 69, P = 0.119), indicating that baseline connectivity with hippocampal targets rather than with parietal stimulation locations predicted treatment-related changes in fMRI regional interconnectivity.

Regionally constrained analysis for correlation of changes in memory and fMRI connectivity

We used a regionally constrained voxel-based approach to identify relationships between effects of stimulation on memory performance and on fMRI connectivity with the hippocampal target. A search volume was created of voxels that demonstrated at least marginal baseline to Post-Tx connectivity change for stimulation relative to sham (voxel-wise P < 0.05, with no spatial extent threshold). Within this search volume, we performed voxel-wise correlation (Pearson) of stimulation-induced memory change scores (Post-Tx versus baseline for stimulation versus sham) on stimulation-induced change scores for fMRI connectivity with the hippocampal target (Post-Tx versus baseline for stimulation versus sham). To guard against false-positive associations, a spatial extent (i.e., cluster) correction of 202 mm^3 (60 contiguous suprathreshold voxels) was used. Four significant clusters were identified, as shown in Fig. 4B-C. In addition, based on a priori hypotheses of the role of connectivity between hippocampus and the left lateral parietal cortex region that was stimulated in memory, we investigated whether any significant correlation was evident for the treatment-responsive voxels in this region. Indeed, a cluster of 61 mm^3 was identified that showed significant correlation ($R^2_{(adj)} = 0.557$, P = 0.0005 averaged for the cluster; cluster centroid MNI coordinates: -49, -52, +31). Thus, treatment-induced fMRI connectivity increase between lateral parietal cortex and the hippocampal target was significantly correlated with the treatment-induced increase in associative memory performance, but with subthreshold size for the correction applied to the main analysis.

Supplementary analysis of fMRI connectivity among regions of the hippocampal network

We performed an additional analysis to investigate at the voxel level specifically those brain regions with highest versus lowest baseline connectivity with hippocampus in order to test for convergence with the analysis that used anatomical (AAL) labels. As in the AAL-based analysis, we explored fMRI connectivity among regions of the hippocampal network demonstrating at least a marginal baseline to Post-Tx fMRI connectivity change (voxel-wise P < 0.05). These voxels were classified as “In Network” if they were among the top voxels with most robust baseline fMRI connectivity values ($t_{(15)}$>5.1; 2132 voxels) with the hippocampal target and as “Out Network” if they were among the voxels with least robust baseline fMRI connectivity values ($t_{(15)}$<1.6; 2109 voxels) with the hippocampal target (Fig. S3). A full connectivity matrix was then constructed by cross-correlating (Pearson’s) all 4241 time courses with each other and comparing changes in average network connectivity values between and among these networks for Post-Tx versus baseline for stimulation relative to sham. Statistics were calculated using paired T tests, correcting for multiple comparisons using the Bonferroni correction. Three comparisons were made: 1) average connectivity values between only voxels in the In Network, 2) average connectivity values between only voxels in the Out Network, and 3) average

connectivity values between voxels in the In Network with those in the Out Network (see Fig. S3). Compared to sham, stimulation (Post-Tx versus baseline) increased mean interconnectivity of In-Network voxels ($T_{(15)} = 6.60$, $P < 0.0001$, corrected $\alpha = 0.017$ for 3 comparisons) as well as connectivity of In-Network voxels with Out-Network voxels ($T_{(15)} = 6.30$, $P < 0.0001$). Stimulation did not robustly increase interconnectivity of Out-Network voxels ($T_{(15)} = 1.83$, $P = 0.088$). For visualization purposes, only AAL regions with at least ten suprathreshold voxels were displayed in Fig. S3 (all regions entered statistical tests).

Negative-control Experiment

To evaluate whether nonspecific effects of brain stimulation could have produced the effects on fMRI connectivity and associative memory performance reported for the main experiment, we performed a negative-control experiment. rTMS was performed using the same parameters as in the main experiment, but instead of stimulating lateral parietal cortex, the thumb/hand area within primary motor cortex was stimulated. This region is not part of hippocampal resting-state fMRI connectivity networks and did not show robust fMRI connectivity with hippocampus in our sample. Data were collected from eight subjects (5 females, ages 21-32 years) who participated in a 1-week version of the experiment involving the same order of baseline, Mid-Tx, and Post-Tx assessments as in the same experiment, and suprathreshold (100% motor threshold) rTMS to the thumb/hand area, which was identified by MRI and TMS in each subject. The stimulation location was the location at which stimulation caused contraction of the *abductor pollicis brevis*. rTMS to this location was associated with repetitive contraction of the hand/arm muscles that was salient to subjects. One additional subject withdrew from the experiment due to discomfort experienced during the first stimulation session, and no data were included from this subject.

We found no significant change in associative memory for the Post-Tx versus baseline assessment (Fig. S4A; $T_{(7)} = 0.46$, $P = 0.659$). To determine whether this null finding resulted from insufficient power, we performed the same test using only the eight subjects from the main experiment who received suprathreshold stimulation of lateral parietal cortex for the first week of the experiment. For these subjects, the Post-Tx versus baseline change in associative memory was reliable (Fig. S4A; $T_{(7)} = 2.67$, $P = 0.031$). In contrast, the eight subjects who received sham for the first week of the main experiment did not show significant change ($T_{(7)} = 0.57$, $P = 0.585$). Effects of stimulation on associative memory were thus specific to lateral parietal cortex, and did not result for stimulation of motor cortex, given matched power. Further, the fact that stimulation improved memory for the eight subjects who received stimulation during the first week of the main experiment but not those who received sham further supports the specificity of effects by arguing against any placebo-like effect on associative memory. That is, subjects could only determine the condition for each week via comparison with the other week (see above), and therefore subjects were blinded to condition during the first week and therefore not susceptible to placebo-like effects.

Likewise, effects of stimulation on fMRI connectivity were specific to stimulation of lateral parietal cortex in the main experiment. We used an ROI approach to investigate the effects of stimulation for the four regions identified in the main experiment as treatment-responsive (Fig. 2A). Relative to the hippocampal target, fMRI connectivity did not significantly increase for Post-Tx versus baseline for these regions for the motor cortex stimulation group ($T_{(7)} = -1.01$, $P = 0.348$; averaged across all voxels in the four regions). In contrast, fMRI connectivity did increase significantly for the eight subjects receiving stimulation of lateral parietal cortex during the first week in the main experiment (Fig. S4B; $T_{(7)} = 2.90$, $P = 0.023$), but not for the eight subjects who received sham during the first week in the main experiment ($T_{(7)} = -2.26$, $P = 0.058$, Note: marginally significant decrease). The average fMRI connectivity change values are provided in

Fig. S4B. Thus, as for associative memory, changes in fMRI connectivity with the hippocampal target only occurred for stimulation of lateral parietal cortex.

References for Supplementary Materials

27. Rossi S, *et al.* Safety, ethical considerations, and application guidelines for the use of transcranial magnetic stimulation in clinical practice and research. *Clin Neurophysiol* **120**, 2008-2039 (2009).

28. Cox RW. AFNI: Software for analysis and visualization of functional magnetic resonance neuroimages. *Comput Biomed Res* **29**, 162-173 (1996)

29. Voss JL, Hauner KK, Paller KA. Establishing a relationship between activity reduction in human perirhinal cortex and priming. *Hippocampus* **19**, 773-778 (2009)

30. Ruohonen J, Ilmoniemi RJ. Physical principles for transcranial magnetic stimulation. In A. Pasqual-Leone, N.J. Davey (Eds.), Handbook of TMS. Oxford University Press, New York, pp. 18-29 (2002).

31. Althoff RR, Cohen NJ. Eye-movement-based memory effect: A reprocessing effect in face perception. *J Exp Psychol Learn Mem Cogn* **25**, 997-1010 (1999).

32. Weintraub S, *et al.* Cognition assessment using the NIH Toolbox. *Neurology* **12**, S54-64 (2013).

33. Romine CB, Reynolds CR. Sequential memory: A developmental perspective on its relation to frontal lobe functioning. *Neuropsychol Rev* **14**, 43-64 (2004).

34. DeVito LM, Eichenbaum H. Memory for the order of events in specific sequences: Contributions of the hippocampus and medial prefrontal cortex. *J Neurosci* **31**, 3169-3175 (2011).

35. Cella D, *et al.* Neuro-QOL: Brief measures of health-related quality of life for clinical research in neurology. *Neurology* **78**, 1860-1867 (2012).

36. Power JD, Barnes KA, Snyder AZ, Schlaggar BL, Petersen SE. Spurious but systematic correlations in functional connectivity MRI networks arise from subject motion. *Neuroimage* **59**, 2142-2154 (2012).

37. Holmes CJ, *et al*. Enhancement of MR images using registration for signal averaging. *J Comput Assist Tomogr* **22**, 324-333 (1998).

38. Tzourio-Mazoyer N, *et al*. Automated anatomical labeling of activations in SPM using a macroscopic anatomical parcellation of the MNI MRI single-subject brain. *Neuroimage* **15**, 273-289. (2002).

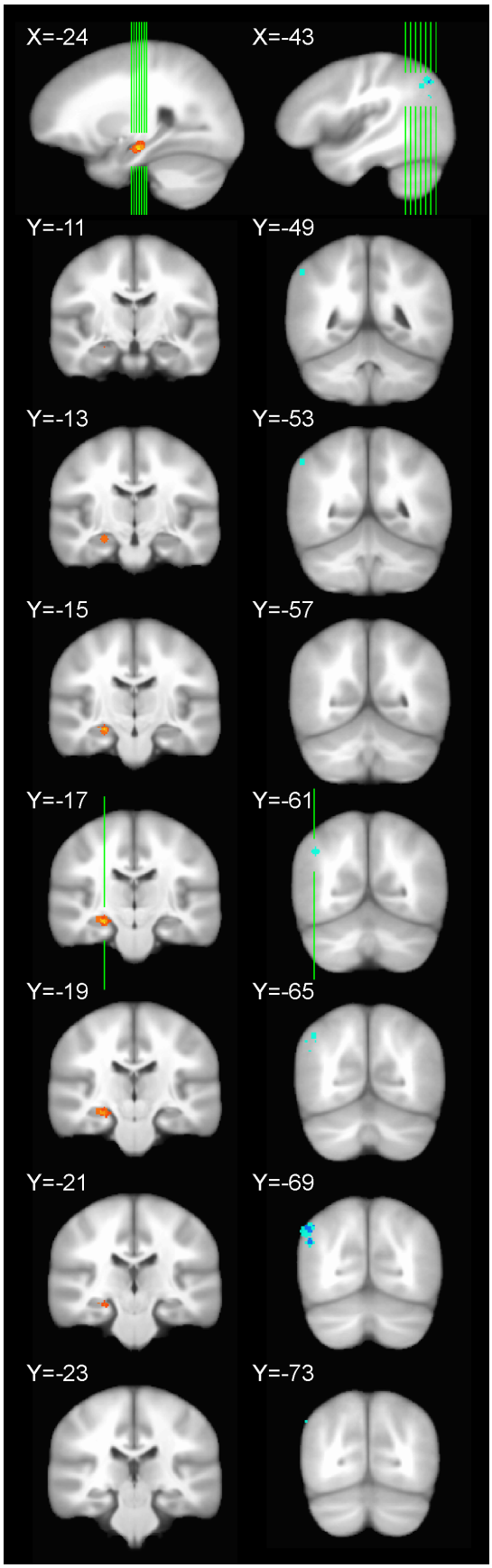

Fig. S1: Hippocampal targets and stimulation locations. Individualized hippocampus targets and parietal cortex stimulation locations are shown in stereotactic space superimposed on a template brain (ICBM452). Voxels in red to yellow indicate location of hippocampal targets, averaged over subjects, with yellow indicating greater across-subject spatial overlap (left column). Voxels in cyan to blue indicate the location of parietal cortex stimulation locations averaged over subjects, with dark blue indicating greater across-subject spatial overlap (right column). The location of the axial slices is indicated by green lines in the sagittal slice at the top of each column.

Fig. S2: Additional detail for Fig. 3. (A) Color labels for Fig. 3A. **(B)** Alternate presentation of Fig. 3A. The matrix depicts links that are significant at P < 0.05 after FDR correction for multiple comparisons in grayscale, with increasing white coloration indicating increasing significance, and non-significant links in black. The matrix is ordered and color-coded by region as in Fig. 3. *FG, Frontal Gyrus; Oper, Pars Opercularis; Tri, Pars Triangularis; Orb, Pars Orbitalis; Supp, Supplementary; TG, Temporal Gyrus; OG, Occipital Gyrus; PL, Parietal Lobule.*

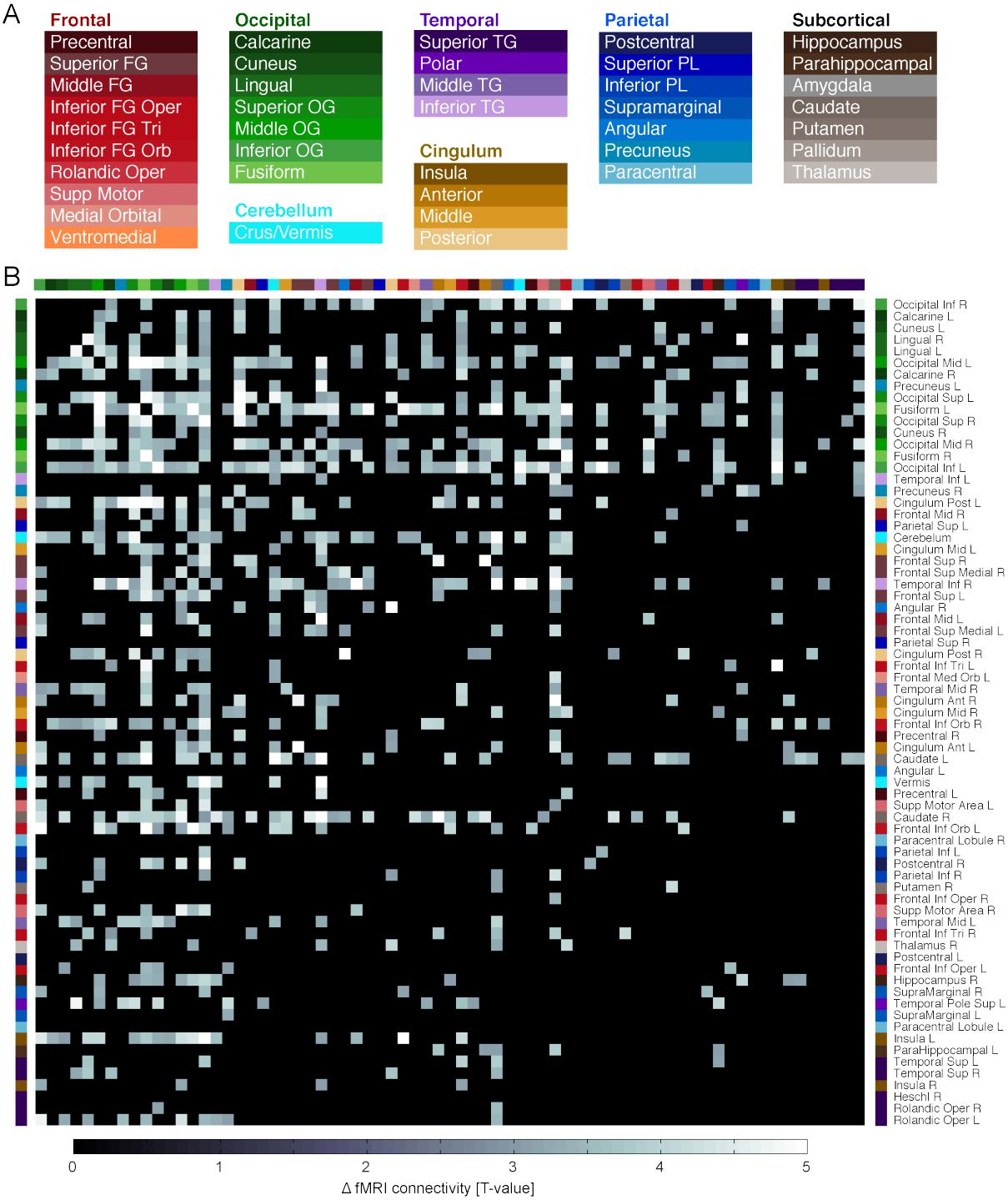

Fig. S3. Supplementary analysis of fMRI regional interconnectivity. (A) Yellow spheres indicate locations of In Network nodes and red spheres indicate locations of Out Network nodes. (**B**) Connectivity change (Post-Tx versus baseline for stimulation versus sham) for the voxels indicated in (A).

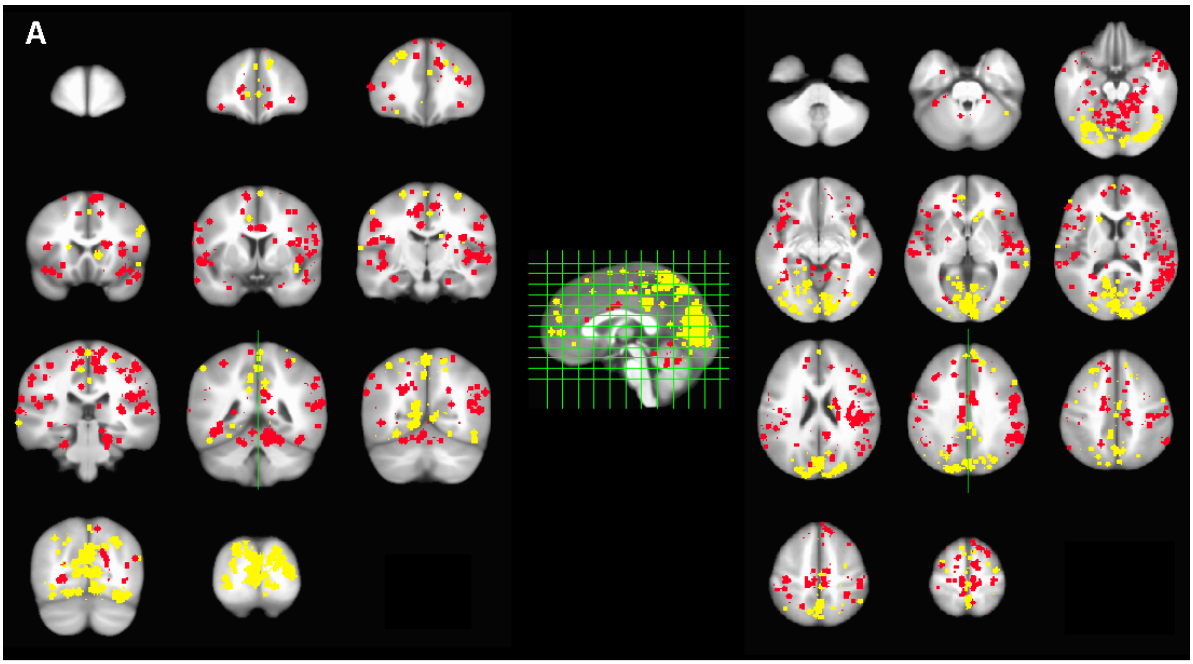

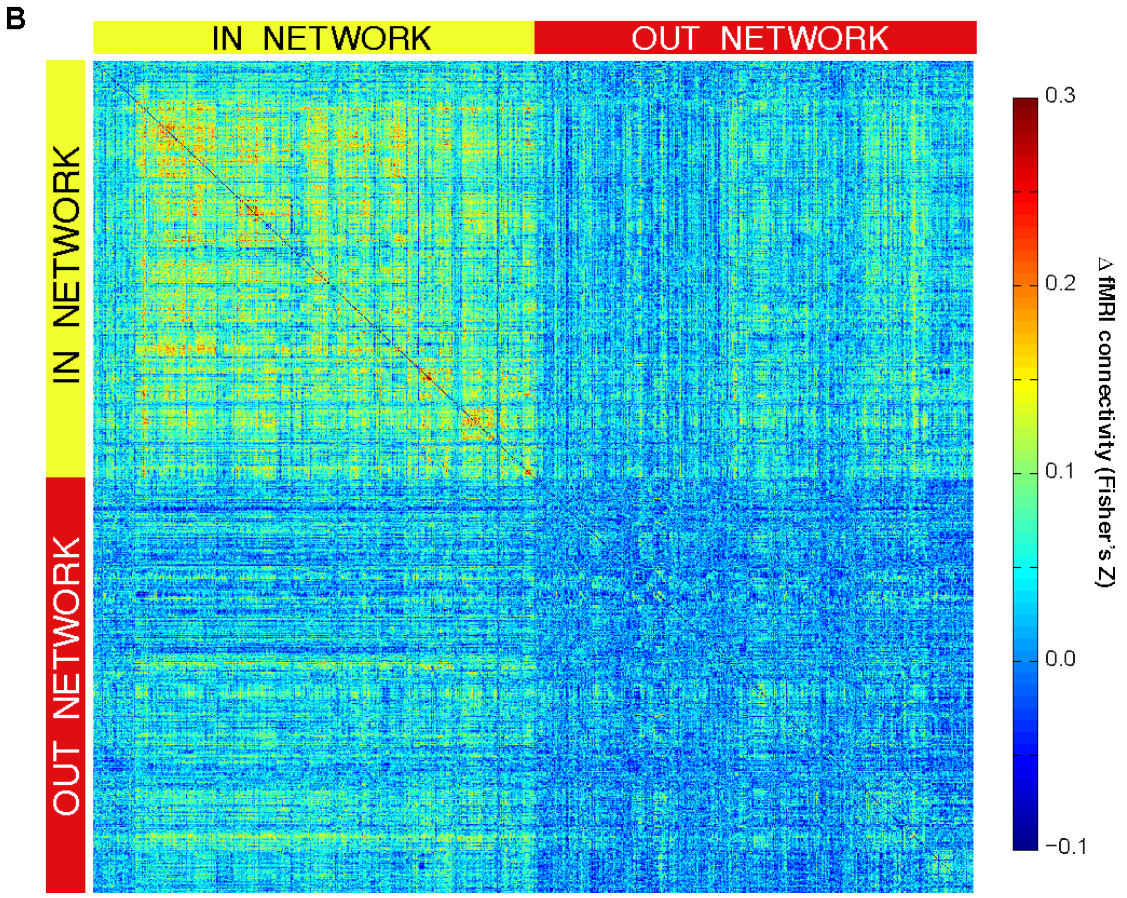

Fig. S4: Findings for the motor-cortex stimulation (negative-control) experiment. (**A**) Change in associative memory performance for Post-Tx versus baseline for subjects receiving motor-cortex stimulation in the control experiment (N=8) and for two conditions and groups of subjects from the main experiment: stimulation for subjects receiving stimulation during week 1 (n=8) and sham for subjects receiving sham during week 1 (n=8). (**B**) Change in connectivity for Post-Tx versus baseline with respect to hippocampal targets, identified for each subject as in the main experiment, averaged for the treatment-responsive regions identified in Fig. 2A, for the same conditions/groups as in (A). *P < 0.05 versus zero, 2-tailed.

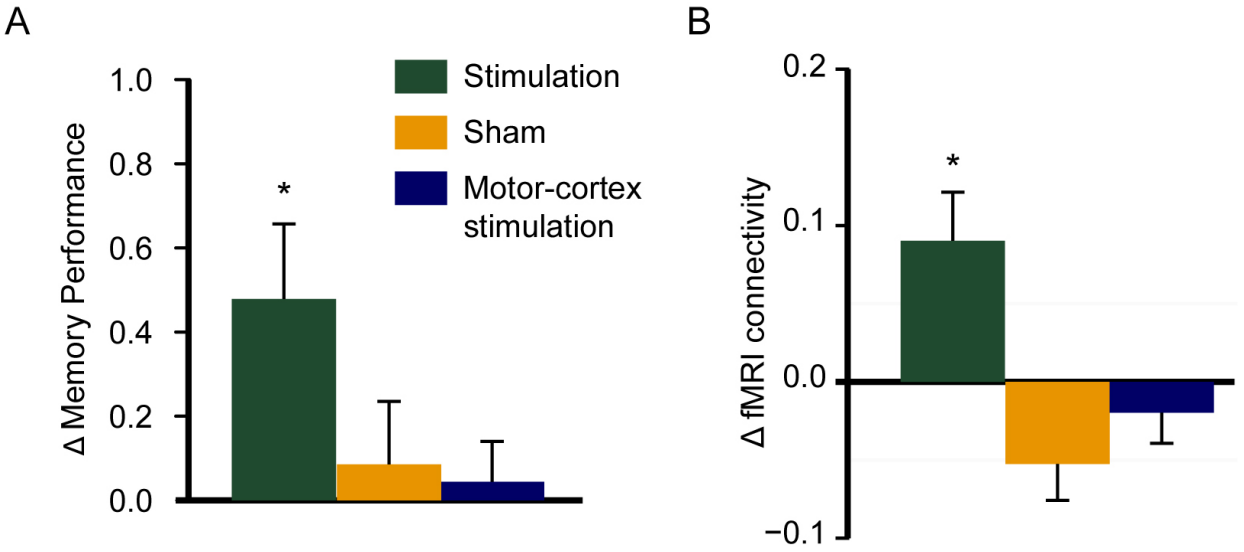

Table S1.

Summary of fMRI connectivity findings for the Post-Tx versus baseline, stimulation versus sham comparison (Fig. 2A), including MNI-305 coordinates of the centroid (mm), volume (mm^3), and approximate Brodmann Area(s) for the cluster centroid (BA).

	Coordinates				
	X	Y	Z	Volume (mm^3)	BA
Retrosplenial cortex and precuneus (bilateral)*	-2	-76	+20	18,039	18/31
Fusiform and parahippocampal cortex (bilateral)**	+13	-66	-23	2,933	18/19
Superior parietal lobule (left)	-30	-51	+57	1,283	40/7
Lateral parietal cortex (left)§	-52	-54	+33	975	40

*This region also includes cuneus and posterior cingulate cortex.

**This region also includes the most superior aspect of cerebellum adjacent to fusiform cortex.

§ P = 0.05

Table S2.

Associative memory performance, provided as mean raw scores (numbers of words correctly recalled to associated face cues) and as mean raw change scores (i.e., not as a proportion of baseline, as in the primary analyses presented in Fig. 4A) relative to each baseline assessment calculated for each subject. Parentheses indicate standard error of the mean.

	Raw scores	Raw change from baseline
Stimulation		
Baseline	8.88 (0.79)	0
Mid-Tx	8.75 (0.83)	-0.13 (0.60)
Post-Tx	10.75 (0.62)	1.88 (0.47)
Sham		
Baseline	10.19 (1.09)	0
Mid-Tx	9.19 (0.95)	-1.00 (0.69)
Post-Tx	10.19 (0.96)	0.00 (0.71)